Journal of Medicinal Chemistry Article

J. Med. Chem. **2010,** *53,* 1979–1989 **1979**
DOI: 10.1021/jm901649x

Structure-Based Design, Synthesis, and Biological Studies of New Anticancer Norindenoisoquinoline Topoisomerase I Inhibitors

Yunlong Song,[†,‡,∥] Zhiyu Shao,[†,∥] Thomas S. Dexheimer,[§] Evan S. Scher,[§] Yves Pommier,[§] and Mark Cushman*[,†]

[†]*Department of Medicinal Chemistry and Molecular Pharmacology, School of Pharmacy and Pharmaceutical Sciences, and the Purdue University Center for Cancer Research, Purdue University, West Lafayette, Indiana 47907,* [‡]*Department of Medicinal Chemistry, School of Pharmacy, Second Military Medical University, Shanghai 200433, China, and* [§]*Laboratory of Molecular Pharmacology, Center for Cancer Research, National Cancer Institute, National Institutes of Health, Bethesda, Maryland 20892.* [∥]*These authors contributed equally to this work.*

Received August 1, 2009

On the basis of the superimposition of the crystal structures of norindenoisoquinoline **5** and topotecan (**2**) bound in the topoisomerase I−DNA covalent complex, as well as molecular docking and quantum chemical calculations, the substituted norindenoisoquinoline **14a** was designed by transporting the 9-dimethylaminomethyl group of topotecan to the 10-position of the norindenoisoquinoline **5**. The desired compound **14a** was synthesized and found to possess topoisomerase I inhibitory activity that was slightly better than that of the starting compound **5**. A focused set of 10-substitued norindenoisoquinoline analogues were then synthesized. The imidazole-substituted compound **14c** was highly cytotoxic when evaluated in a series of human leukemia, ovarian, and breast cancer cells.

Introduction

DNA topoisomerase I (Top1[a]) has become an important target for the design of novel antitumor drugs.[1] It is a ubiquitous and essential nuclear enzyme for DNA replication and transcription.[2] As a class, the Top1 inhibitors in the camptothecin (CPT, **1**; Chart 1) family have historically suffered from poor water solubility, high toxicity, and metabolic instability.[3] Therefore, substantial efforts were made to improve the water solubilities, toxicity profiles, and pharmacokinetics of CPT derivatives. These efforts were eventually rewarded by the development of the two clinically useful, water-soluble CPT derivatives topotecan (**2**) and irinotecan (**3**).[4]

However, the clinically useful CPTs are not ideal drug molecules because they are compromised by the following inherent limitations: (1) the E-ring of CPT contains an α-hydroxylactone that opens to a hydroxycarboxylate that binds tightly to serum albumin;[5,6] (2) the drug−target interaction is reversible and has to be maintained long enough to convert Top1 cleavage complexes into DNA damage;[7] (3) several Top1 resistance mutations such as Asn722Ser and Arg364His occur;[8,9] (4) tumor cells that overexpress drug efflux pumps are resistant to CPTs;[10] (5) the side effects caused by camptothecins limit the doses that can be safely administered and, therefore, antitumor efficacy.[11−13]

To overcome the lactone instability, reversibility of the drug−target interaction, and drug resistance, extensive efforts have been made to discover non-CPT Top1 inhibitors that share similar specificities and potencies with CPT, yet display unique pharmacokinetics, toxicity profiles, and resistance characteristics.[1,11,13−17] Several types of non-CPT Top1 inhibitors, including the indolocarbazoles and indenoisoquinolines, have been reported.[17,18] The discovery of the prototypical indenoisoquinoline NSC314622 (**4**) as a Top1 inhibitor originated from a COMPARE analysis.[19] Significant progress has been made on the improvement of the potencies of the indenoisoquinolines through structure manipulation.[20−33] Several indenoisoquinoline compounds such as indimitecan (NSC 725776) and indotecan (NSC 724998) produce persistent Top1 cleavage complexes and overcome multidrug resistance.[34]

During the synthetic modification of the indenoisoquinolines, a norindenoisoquinoline AI-III-52 (**5**) was discovered that demonstrated very high cytotoxicities in the NCI in vitro anticancer screen (mean graph midpoint of 50 nM) and strong Top1 inhibitory potency.[35] The DNA cleavage patterns of norindenoisoquinolines are somewhat different from those of the widely studied indenoisoquinolines. These important differences indicate that different cancer cell genes could be targeted more selectively with one type of inhibitor vs another. Similar to the situation with Top2 or tubulin inhibitors that share a single target, it can be expected that different Top1 inhibitors will have different spectra of anticancer activity. Furthermore, norindenoisoquinoline **5** was observed by X-ray crystallography to adopt a "flipped" orientation (relative to indenoisoquinolines) in its ternary cleavage complex.[35,36] The binding of the norindenoisoquinolines in the Top1−DNA complex has been determined by high level ab initio quantum chemical studies to be mainly governed by $\pi-\pi$ stacking forces.[37] The data clearly indicate that the norindenoisoquinolines are novel Top1 inhibitors. However, their solubility limitations have hindered further preclinical development. This situation has dictated the challenging task of designing and synthesizing novel highly potent norindenoisoquinolines with enhanced water solubility.

*To whom correspondence should be addressed. Phone: 765-494-1464. Fax: 765-494-6790. E-mail: cushman@purdue.edu.

[a] Abbreviations: ADME, absorption, distribution, metabolism, and excretion; AIBN, azobisisobutyronitrile; BSA, bovine serum albumin; CPT, camptothecin; EDTA, ethylenediaminetetraacetic acid; MGM, mean graph midpoint; NBS, *N*-bromosuccinimide; QM, quantum mechanics; SDS, sodium dodecyl sulfate; TEA, triethylamine; Top1, topoisomerase I.

Published on Web 02/15/2010

Chart 1. Chemical Structures of Representative Top1 Inhibitors

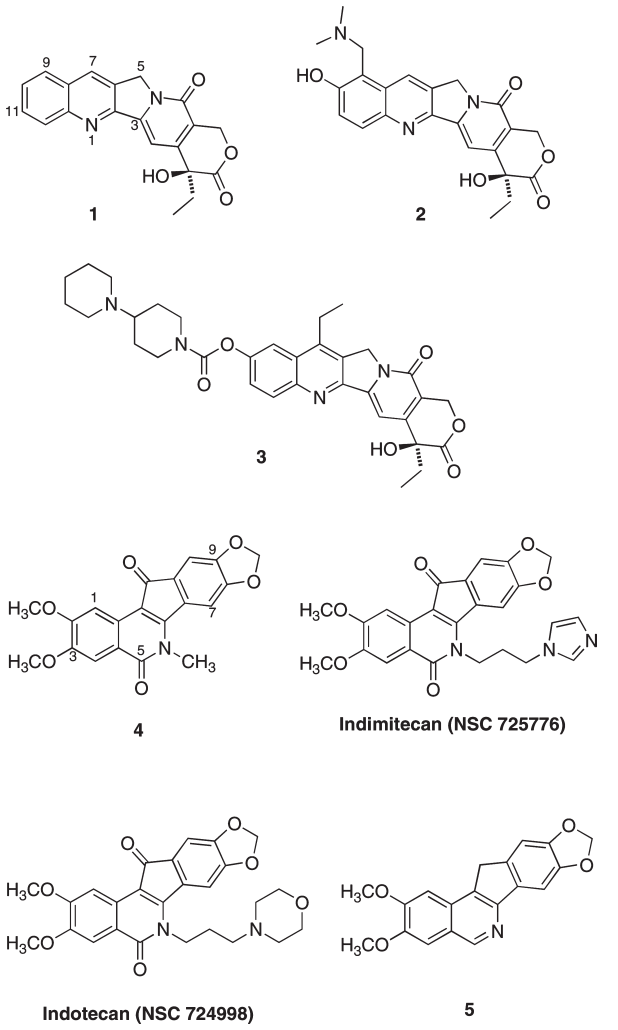

Fortunately, the X-ray crystal structures of ternary complexes containing Top1 and a DNA fragment binding to several different Top1 inhibitors have been reported. These include ternary complexes derived from camptothecin,[38] topotecan,[39] indolocarbazole,[38] indenoisoquinoline,[38] and norindenoisoquinoline[35] Top1 inhibitors. This provides a strong structural basis for the rational design of highly potent norindenoisoquinolines with enhanced water solubility.

Herein, the structure-based design, chemical synthesis, and in vitro cytotoxic evaluations of novel potent norindenoisoquinolines with enhanced water solubility are reported. The present study was also conducted to assess the contributions of different representative nitrogen-containing side chains on the 10-position of norindenoisoquinoline to their cytotoxic properties and Top1 inhibitory activities. This has also demonstrated the power of fragment-based design combined with computational chemistry to advance the structure-based drug design process.

Results and Discussion

Molecular Design. The crystal structures of Top1−DNA−inhibitor complexes allow the superimposition of the inhibitors in the ternary complexes.[35,38,39] That, in turn, can suggest the migration of effective substituents from a region of one inhibitor to a spatially equivalent location on a different inhibitor. This "mix-and-match" strategy can suggest the rational exchange of substituents among Top1 inhibitors in order to maximize substituent effects. In the present study, the two crystal structures **5**−DNA−Top1 (PDB code 1tl8)[35] and topotecan **2**−DNA−Top1 (PDB code 1k4t)[39] were superimposed on the basis of all the heavy atoms of the protein, as portrayed in Figure 1.

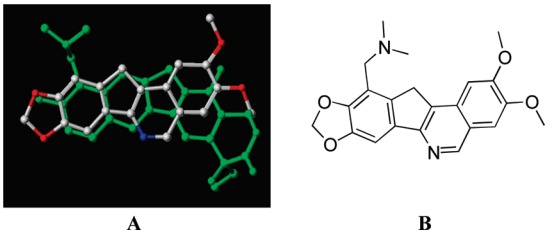

Figure 1. (A) Overlap of norindenoisoquinoline **5** vs topotecan (**2**) based on the superimposition of the target enzyme. (B) Proposed water-soluble norindenoisoquinoline compound **14a**.

As seen from the overlapped crystal structures, the 9-position of topotecan (**2**) overlaps with the 10-position of the indenoisoquinoline ring system (see structures **1** and **4** for atom numbering scheme). Attachment of the 9-dimethylaminomethyl substituent of topotecan (**2**) to the 10-position of the norindenoisoquinoline **5** results in the potential Top1 inhibitor **14a** displayed in Figure 1B, which is expected to have increased polarity, and could be formulated as a hydrochloride salt. The design of **14a** was also corroborated by molecular docking studies, in which **14a** displayed better docking scores and more favorable calculated binding energy than **5** (see Supporting Information). Furthermore, since substituents on the 10-position of the norindenoisoquinolines and the 7-position of the indenoisoquinolines project similarly into the DNA major groove, the 10-dimethylaminomethyl substituent of the compound in Figure 1B might be advantageously swapped with the types of 7-position substituents of the indenoisoquinolines that have been shown to confer greater Top1 inhibitory activity. This strategy might result in favorable interactions of the inhibitors with the Top1−DNA covalent complex and thus enhance antitumor activity.

A further goal of the present study was to investigate the structure−activity relationships (SAR) of 10-position nitrogen-containing side chains and optimize ADME properties. Starting from **14a**, a focused set of 10-substituted norindenoisoquinolines were designed. All the resulting structures were docked into the Top1−DNA covalent complex, and only those with better docking scores and more favorable calculated binding energies were kept for further synthesis. This resulted in norindenoisoquinolines **14b**−**f**.

Quantum Chemistry. As described above, a methylene linker was chosen for **14a** and its derivatives. 9-Methyl-CPT, in which the 9-methyl group occupies space that overlaps with the 10-methylene group of the norindenoisoquinolines in the ternary complex, was reported to demonstrate better Top1 inhibition than CPT.[40] A quantum chemical investigation was therefore considered to answer the question of whether a 10-methyl group would increase the binding of the norindenoisoquinoline system to DNA as has been shown with 9-methyl-CPT. High level quantum chemical MP2 calculations were performed on 10-methyl-norindenoisoquinoline **15** using our recently published strategy, and the results were compared with those of norindenoisoquinoline **5** from previous calculations.[37] The attachment of a

Table 1. Interaction and Solvation Energies (kcal/mol) of Norindenoisoquinolines Binding to Simplified Cleavage Complex[37] Calculated by the MP2/6-31G*(0.25) Method

	compd		
parameters	**5**	**15**	**14a**[d]
E_{int} (MP2)[a]	−31.56	−32.87	−31.77*
$\Delta G_{solvation}$(MP2)[b]	−40.25	−38.32	−36.53*
$E_{int} + \Delta G_{solvation}$	−71.81	−71.19	−68.3*
ΔE[c]	0	0.62	3.51*

[a] $E_{int} = E_{complex} - E_{ligand} - E_{bp}$ + BSSE. [b] $\Delta G_{solvation}(MP2) = E_{PCM-MP2} - E_{MP2}$. [c] ΔE was the relative binding energy difference in aqueous solution between **15**, **14a**, and AI-III-52 investigated at the MP2 level, respectively. [d] The 10-position substituent of **14a** forms direct interactions with neighboring Top1 residues which were not included in the MP2 calculations because of impractically high computational cost. Therefore, the values with an asterisk are not meaningful indicators of binding to the DNA−Top1 covalent complex.

Scheme 1[a]

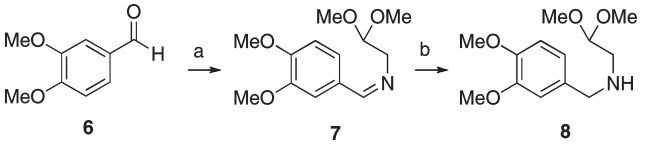

[a] Reagents and conditions: (a) $(MeO)_2CHCH_2NH_2$, PhH, 23 °C (4 h); (b) $NaBH_4$, EtOH, reflux (30 min).

methyl group did contribute −1.31 kcal/mol to the calculated in vacuo binding energy, from −31.56 kcal/mol of norindenoisoquinoline **5** to −32.87 kcal/mol of **15** (Table 1). However, the calculated relative binding energy difference in aqueous solution between **15** (−71.19 kcal/mol) and norindenoisoquinoline **5** (−71.81 kcal/mol) of 0.62 kcal/mol suggests that compound **15** would act as a less potent Top1 inhibitor compared to the norindenoisoquinoline **5**. The QM result suggests that the same substituent may elicit different calculated effects on activity if transferred to a new scaffold (in this case a methyl added to **5** vs CPT) even though it occupies the same space in the binding site.

QM calculations of the binding energy of compound **14a** were also performed. The attachment of a dimethylaminomethyl substituent to **5** contributes −0.21 kcal/mol to the calculated DNA interaction energy, which indicates the attachment of such a bulky group would not interfere with the binding of the scaffold to DNA. However, it should be noted that a simplified DNA cleavage complex, which lacks protein residues, was used in the MP2 calculations because of the high computational cost.[37] Therefore, the calculations involving **14a** cannot be expected to provide an accurate indicator of binding in the ternary complex because the bulky dimethylamino substituent makes direct contact with the neighboring protein residues. On the other hand, the methyl group of **15** only interacts with the DNA fragment in the ternary complex.

Chemistry. The syntheses of the desired compounds **14a**−**f** and **15** are outlined in Schemes 1−3. The general strategy is based on the classical Pomeranz−Fritsch reaction[41] and its improved versions including the Bobbitt[42] and Jackson modifications.[43] The required precursor **8** of the isoquinoline ring system was prepared as outlined in Scheme 1.[35] Condensation of veratraldehyde (**6**) with aminoacetaldehyde dimethyl acetal resulted in formation of the Schiff base **7**, which was reduced to the amine **8** with sodium borohydride in ethanol.

Scheme 2[a]

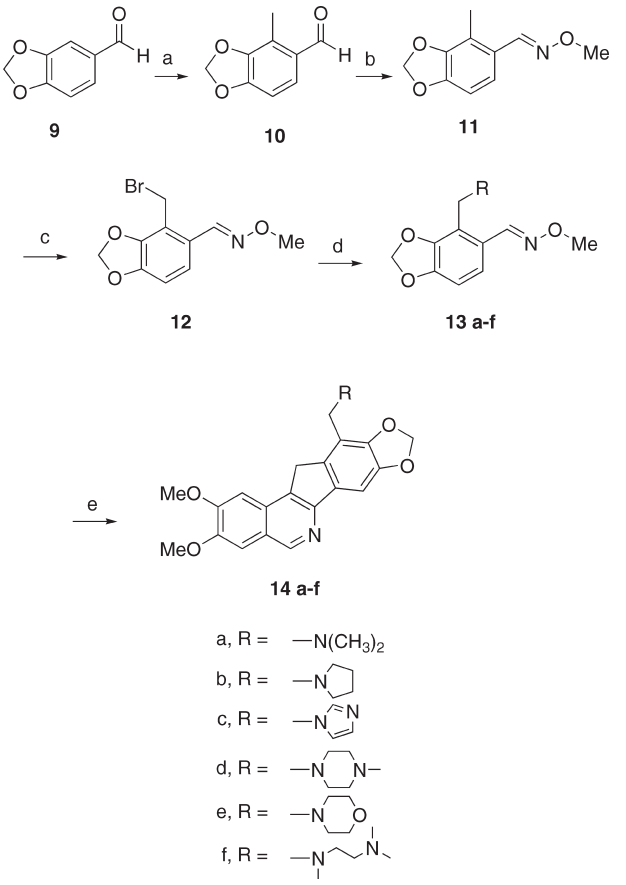

[a] Reagents and conditions: (a) (1) $Me_2NCH_2CH_2NMeLi$, THF, −78 °C (1 h), (2) MeI, −78 °C (2 h); (b) $MeONH_3^+Cl^-$, NaOAc, MeOH, 23 °C (1 h); (c) NBS, AIBN, CCl_4, reflux (3 h); (d) amine, THF, 23 °C; (e) **8**, concd HCl, 100 °C.

Scheme 3[a]

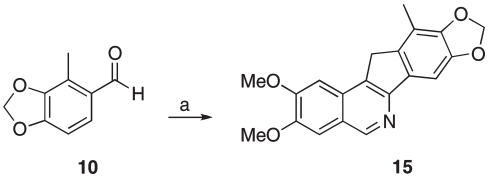

[a] Reagents and conditions: (a) **8**, concd HCl, 100 °C (18 h).

As detailed in Scheme 2, regioselective deprotonation of piperonal (**9**) with lithium *N*,*N*,*N*′-(trimethyl)ethylenediamine in THF resulted in a phenyllithium intermediate that was methylated to afford 2-methylpiperonal (**10**).[44] The aldehyde **10** was converted to its oxime ether **11**, which was subjected to free radical bromination with NBS and AIBN in refluxing carbon tetrachloride to afford the benzyl bromide **12**. Displacement of the bromide with various amines provided the penultimate intermediates **13a**−**f**. Condensation of compounds **13a**−**f** with intermediate **8** in concentrated hydrochloric acid at 100 °C yielded the final products **14a**−**f** in low yields (3.1−7.8%). The reaction mixtures were very complex, and the yields were compromised by formation of uncyclized 4-benzylisoquinolines and by extremely challenging purifications of the final products. Nevertheless, the compounds were eventually obtained in pure form in sufficient quantities for biological testing.

The crystal structure of the norindenoisoquinoline **14a** (Figure 2) provides a reliable starting conformation for the quantum chemical calculations and also constitutes an independent verification of the structure. The inclusion of one molecule of chloroform in the crystal structure is consistent with our long-term experience that solvents are very difficult to remove from indenoisoquinolines in the solid state.

The 10-methylnorindenoisoquinoline **15** was also prepared in order to evaluate the contributions that the amine moieties of **14a**−**f** made to their in vitro cytotoxicities and Top1 inhibitory activities. Condensation of intermediates **8** and **10** under the usual harsh acidic conditions resulted in formation of the desired product **15** (Scheme 3).

Biological Studies. All of the norindenoisoquinolines were examined for antiproliferative activity in the National Cancer Institute's Developmental Therapeutics Program (DTP).[45,46] Each compound was evaluated against approximately 55 human cell lines representing leukemia, melanoma, and cancers of the lung, colon, brain, breast, ovary, prostate, and kidney. After an initial one-dose assay at a single high dose (10^{-5} M), only compounds that satisfied the predetermined threshold inhibition criteria were selected for further five-dose assay. The selected compounds were tested at five concentrations ranging from 10^{-8} to 10^{-4} M. The GI_{50} values from each subpanel were obtained with selected cell lines, and overall antiproliferative effects are quantified as a mean graph midpoint (MGM, Table 2). The MGM is a measure of the average GI_{50} for all of the cell lines tested, in which GI_{50} values below and above the test range (from 10^{-8} to 10^{-4} M) are taken as the minimum (10^{-8} M) and maximum (10^{-4} M) drug concentrations used in the assay. For comparison, the activities previously reported for camptothecin (**1**), indenoisoquinoline **4**, and norindenoisoquinoline (**5**) are also listed in the table.

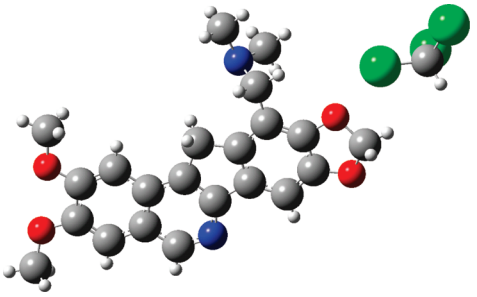

Figure 2. Crystal structure of norindenoisoquinoline **14a** (the neighboring solvent molecule is chloroform).

The introduction of the 10-methyl group into compound **5**, resulting in norindenoisoquinoline **15**, significantly lowered the cytotoxicity about 230-fold according to their respective MGM values. However, the further introduction of basic functional groups into compond **15** increased the cytotoxicity even though it had variable effects on the Top1 inhibitory activity.

The imidazole-substituted norindenoisoquinoline compound **14c** is the most cytotoxic compound in this series, with an MGM of 0.52 μM. Notably, the hydrophobic prototype **5** is inactive in colon HCT-116 cancer cell and renal SN12C cancer cell cultures, whereas compound **14c** is potent against these two tumor cell types, with GI_{50} values of 0.16 and 0.60 μM, respectively. All of the 10-aminomethylene norindenoisoquinolines except **14f** demonstrated good activity against these two tumor cell lines. The 10-aminomethylene norindenoisoquinolines have different anticancer spectra compared to their hydrophobic counterpart **5**. As norindenoisoquinoline **14c** was the most cytotoxic in the series, yet demonstrates moderate Top1 inhibition, additional cellular targets mediating the cytotoxic effects possibly exist.[35]

Norindenoisoquinoline **14c** was highly cytotoxic against a selected series of human cancer cells, especially against leukemia, breast, and ovarian cancer cells (Table 3). The GI_{50} values of **14c** against leukemia SR, CCRF-CEM, RPMI-8226, and MOLT-4 are 12, 37, 41, and 60 nM, respectively. It also displayed strong cytotoxicity against the human breast cancer cell MCF-7 with a GI_{50} of 90 nM. This compound demonstrated a GI_{50} of 121 nM against human ovarian cancer cell IGROVI. Clearly, the norindenoisoquinoline **14c** represents an interesting chemical entity that merits further preclinical investigation.

Norindenoisoquinolines **5**, **14a**−**f**, and **15** were examined for induction of Top1-mediated DNA cleavage using a 117-bp DNA oligonucleotide encompassing the previously identified Top1 cleavage sites in the 161-bp fragment from pBluescript SK(−) phagemid DNA.[13] The resulting gel electrophoresis DNA cleavage patterns are displayed in Figure 3, along with those resulting from CPT and the indenoisoquinoline **MJ-III-65**.[43] As often found in the case of indenoisoquinoline series of Top1 inhibitors, a close

Table 2. Cytotoxicities and Topoisomerase I Inhibitory Activities of Norindenoisoquinolines

	cytotoxicity (GI_{50} in μM)[a]									
compd	lung HOP-62	colon HCT-116	CNS SF-539	melanoma UACC-62	ovarian OVCAR-3	renal SN12C	prostate DU-145	breast MDA-MB-435	MGM[b]	Top1 cleavage[c]
CPT	0.01	0.03	0.01	0.01	0.22	0.02	0.01	0.04	0.0405	++++
4	1.30	35	41	4.2	73	68	37	96	20	++
5	0.072	>100	<0.01	<0.01	NT[d]	>100	0.028	<0.01	0.050	++(+)
14a	6.7	1.5	14	12	1.4	13	1.6	16	4.4	+++
14b	1.2	0.64	1.9	6.7	0.73	4.4	0.73	2.5	2.3	+++
14c	0.35	0.16	0.28	0.21	0.21	0.60	0.26	NT[d]	0.52	+(+)
14d[e]										++
14e	2.1	1.4	1.8	100	1.7	2.3	1.9	NT[d]	2.4	+
14f	1.5	1.9	11	0.73	7.4	>100	3.4	NT[d]	6.3	+(+)
15	7.3	0.89	4.6	0.70	5.8	>100	>100	>100	11.8	++

[a] The cytotoxicity GI_{50} values are the concentrations corresponding to 50% growth inhibition. [b] Mean graph midpoint for growth inhibition of all human cancer cell lines successfully tested. [c] The compounds were tested at concentrations ranging up to 10 μM. The activity of the compounds to produce Top1-mediated DNA cleavage was expressed semiquantitatively as follows: 0, no activity; +, weak activity; ++, moderate activity; +++, good activity; ++++, similar activity as 1 μM CPT. [d] NT = not tested. [e] Not selected for further testing; refer to text for details.

Table 3. Cytotoxicities of **14c** against a Series of Selected Human Cancer Cells (GI_{50} in μM)

							colon cancer		renal cancer		CNS cancer	
	leukemia	non-small-cell lung cancer	melanoma	ovarian cancer	prostate cancer	breast cancer						
	SR	NCI-H460	UACC-62	IGROVI	DU-145	MCF7	HCC-2998	COLO 205	CAKI-1	ACHN	U251	SF-295
1st run	0.012	0.16	0.21	0.033	0.26	0.09	0.11	0.76	0.17	0.27	0.15	0.16
2nd run		0.11	0.18	0.21	0.41	0.089	2.1	0.28	0.40	0.30	0.17	0.13
mean	0.012	0.13	0.20	0.12	0.33	0.090	1.1	0.51	0.29	0.28	0.16	0.15

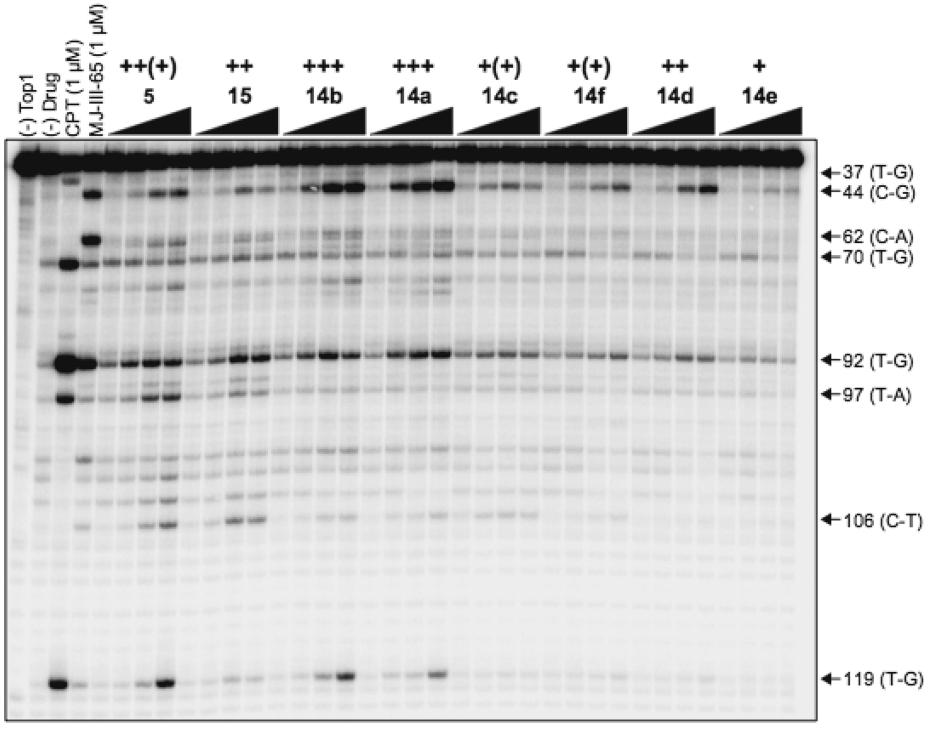

Figure 3. Top1-mediated DNA cleavage induced by norindenoisoquinolines **14a**−**f** and **15**: (lane 1) DNA alone; (lane 2) Top1 alone; (lane 3) camptothecin (**1**), 1 μM; (lane 4) **MJ-III-65**, 1 μM; (lanes 5−36) (for **5**, **15**, **14a**−**f**) Top1 + indicated compound at 0.1, 1, 10, and 100 μM, respectively. The numbers on the right and arrows indicate cleavage site positions. A 117-bp DNA substrate was used in this assay, but the cleavage sites are numbered to be consistent with the 161-bp DNA substrate traditionally used in this assay in order to facilitate comparison.

correlation between Top1 inhibition and antiproliferative activity was not observed.[20−33] Compound **14a** displayed slightly better Top1 inhibition than the starting lead compound, norindenoisoquinoline **5**. However, the cytotoxic activity of **14a** was not as good as expected, which might due to many factors besides the interaction with target enzyme, such as cellular permeability, distribution, and metabolism. Compound **15** has a ++ Top1 inhibition, whereas **5** has a ++(+) Top1 inhibition. This is consistent with the QM prediction that **15** would be a less potent Top1 inhibitor than **5**.

The norindenoisoquinolines produced different DNA cleavage patterns. For example, the 106 (C-T) cleavage observed with norindenoisoquinolines **5** and **15** was absent in **14d** and **14e**. Also, some of the cleavage sites induced with the norindenoisoquinolines more closely resemble the indenoisoquinolines than the camptothecins. For example, the 44 (C-G) cleavage site was seen with the indenoisoquinoline **MJ-III-65** and the norindenoisoquinolines **5**, **14a**−**e**, and **15** but not with CPT, whereas the 37 (T-G) site is observed with CPT but not with the indenoisoquinolines and norindenoisoquinolines.

The DNA cleavage patterns induced by the norindenoisoquinolines share some similarity with indenoisoquinolines, but distinguishing differences also exist. For example, the 62 (C-A) site is observed with **MJ-III-65** while not with the norindenoisoquinolines. The 119 (T-G) site is found in the norindenoisoquinolines **14a**,**b** but not with **MJ-III-65**. Introduction of the 10-position nitrogen-containing side chains seems to result in preferential binding to the 44 (C-G) site in comparison with the hydrophobic norindenoisoquinolines **5** and **15**. The 97 (T-A) site observed in **5** and **15** is hardly detected in the norindenoisoquinolines **14a**−**e**. These observations are important because they indicate that there could be selectivity in cancer gene targeting with the norindenoisoquinolines vs indenoisoquinolines and CPT. It can therefore be expected that different Top1 inhibitors may selectively target different tumor types.

Molecular Modeling. The pK_a values of the amines **14a**−**f** were calculated to determine the dominant species at physiological pH 7.4 using the online program ADME Boxes (http://www.pharma-algorithms.com/webboxes/) from Pharma Algorithms, which has been described as "the most predictive, high throughput pK_a predictor" based on a recent comparison of current in silico pK_a prediction tools by Balogh et al.[47] The method employs the pK_a prediction tool of Pharma Algorithms used in the present study. The algorithm utilizes ~18000 experimental pK_a data points, a database of

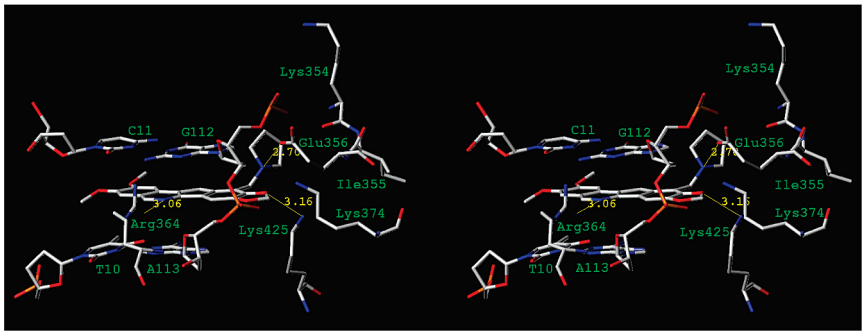

Figure 4. Binding model of **14b** binding to Top1−DNA cleavage complex.

~4600 ionization centers, ~500 interaction constants, and four interaction calculation methods to produce microconstants. In addition, the log *P* and log *D* values were also calculated with the Pharma Algorithms online service, and the data are included in the Supporting Information. From the data, it is clear that by the introduction of 10-position nitrogen-containing side chain substitutions, the log *D* values were decreased significantly. Obviously, the aqueous solubilities of **14a**−**f** can be further enhanced through salt formation, and in fact clear aqueous solutions of hydrochloride salts were observed during workup of the reaction mixtures that produced these products.

From the data, the two most potent compounds **14a** and **14b** against Top1 have tertiary amines with pK_a values of about 8.6. This pK_a value means the nitrogen atom attached to 10-benzyl group of norindenoisoquinoline is 95% protonated at physiological pH. The dominant species of **14d** and **14f** are monoprotonated on their distal nitrogens. For compounds containing two nitrogen atoms such as piperazine, one nitrogen atom is protonated first, making the other nitrogen less basic. For example, the pK_a values of piperazine are 9.81 and 5.59, respectively.[45] As for **14c** and **14e**, the dominant species are unprotonated forms (88% and 95%, respectively) at physiological pH.

To further explore the influence of protonation states of **14a** and **14b** on Top1 inhibition, the protonated form and also the free bases of these two compounds were docked into Top1−DNA covalent complex (PDB code 1tl8). Clearly, the protonated species is calculated to form stronger interactions with the Top1−DNA covalent complex compared to the free bases. For example, in Figure 4, the "additional" hydrogen atom attached to the pyrrolidine nitrogen atom forms a direct hydrogen bond with Glu356 of Top1. Moreover, the isoquinoline nitrogen atom at the 6-position of the norindenoisoquinoline forms a characteristic hydrogen bond with Arg364 and one oxygen atom of the methylenedioxy group neighboring the 10-position of norindenoisoquinoline forms a hydrogen bond with Lys425.

The most potent compound **14c** exists predominantly in its neutral form (88%) at physiological pH based on calculated pK_a values. From molecular docking studies, the neutral form afforded a less favorable binding energy (−71.7130 kcal/mol) than all the other nitrogen-containing side chain substituted norindenoisoquinolines (Supporting Information). This is consistent with the Top1 inhibition data that **14c** is a poor Top1 inhibitor. On the other hand, compound **14c** exhibited high cytotoxicity, indicating that additional molecular targets likely exist for this compound.

Conclusions

10-Substituted norindenoisoquinolines with improved aqueous solubilities were designed and synthesized. The design was based on superimposition of two crystal structures of norindenoisoquinoline **5** and topotecan (**2**) binding to the Top1−DNA covalent complex, molecular docking, and quantum mechanics studies. The 10-dimethylaminomethyl norindenoisoquinoline **14a** was designed by moving the 9-dimethylaminomethyl group of topotecan to the 10-position of the norindenoisoquinoline, resulting in slightly better Top1 inhibition relative to the parent compound **5**. Molecular docking studies subsequently led to the design of a focused set of 10-substituted norindenoisoquinolines **14b**−**e**. Among them, the imidazole-substituted compound **14c** demonstrated nanomolar cytotoxicity against a series of human leukemia, ovarian, and breast cancer cells and is worthy of further preclinical investigation. The new norindenoisoquinolines **14a**−**e** and **15** act as Top1 poisons, stabilizing the Top1−DNA cleavage complex by inhibiting the religation reaction. The pattern of DNA cleavages observed with the norindenoisoquinolines was different from the indenoisoquinolines and camptothecins, suggesting one possible explanation for the unique cytotoxicity profiles observed in each case (e.g., compare cytotoxicity data for camptothecin, indenoisoquinoline **4**, and the norindenoisoquinoline **5** in Table 2). The mean graph midpoint (MGM) values of the norindenoisoquinolines **14a**−**c**, **14e**, **14f**, and **15** are obviously higher than those of camptothecin (**4**) and the previously reported norindenoisoquinoline **5**. However, the new norindenoisoquinolines are significantly more cytotoxic than **5** in selected cell lines (e.g., **14a**−**c**, **14e**, **14f**, and **15** vs colon HCT-116 and **14a**−**c**, **14e** vs renal SN12C cells, Table 2). With regard to the general topic of overall relative cytotoxicities (MGM values), it is worth noting that the Top1 inhibitor indotecan, which has outperformed many of the more cytotoxic indenoisoquinolines in animal models and is presently undergoing clinical trials in cancer patients at the National Cancer Institute, has a relatively unimpressive MGM of 4.64 μM.[17,31] This seems to indicate the possibility that, in some cases, MGM values are being overemphasized when decisions are made in the anticancer drug development process.

The novelty and significance of this work stem from testing a hypothetical design strategy based on exchange of optimized fragments that occupy the same space in the ternary drug−DNA−enzyme complexes.

Experimental Section

Melting points were determined in capillary tubes and are uncorrected. Infrared spectra were obtained using KBr pellets

and were recorded using a Perkin-Elmer 1600 series FTIR. Except where noted, ^{1}H NMR spectra were obtained using $CDCl_3$ as solvent and the solvent peak as internal standard. ^{1}H NMR spectra were determined at 300 MHz on a Bruker ARX-300 spectrometer. Electrospray mass spectra were obtained using a FinniganMATT LCQ (Thermoquest Corp., San Jose, CA). Microanalyses were performed at the Purdue University Microanalysis Laboratory. Most chemicals and solvents were analytical grade and used without further purification. Commercial reagents were purchased from Aldrich Chemical Co. Purities of ≥95% were established by elemental analysis except for compound **14f**, which was estimated to be ≥95% pure by HPLC.

(3,4-Dimethoxybenzylidene)(2,2-dimethoxyethyl)amine (7). 3,4-Dimethoxybenzaldehyde (12.20 g, 73.42 mmol) was dissolved in benzene (200 mL), and aminoacetaldehyde dimethyl acetal (12.0 mL, 11.7 g, 111 mmol) was added. The mixture was stirred at reflux for 4 h using a Dean−Stark trap. The reaction mixture was then concentrated and dissolved in $CHCl_3$ (250 mL). The solution was washed with water (4 × 150 mL) and brine (150 mL), dried (Na_2SO_4), and concentrated, and the last traces of solvent were removed under vacuum to provide the imine (18.41 g, 99.1%) as a light-yellow solid: mp 50−52 °C. ^{1}H NMR (300 MHz, $CDCl_3$) δ 8.18 (s, 1 H), 7.42 (s, 1 H), 7.15 (d, J = 8.4 Hz, 1 H), 6.86 (d, J = 8.4 Hz, 1 H), 4.65 (t, J = 5.1 Hz, 1 H), 3.92 (s, 3 H), 3.90 (s, 3 H), 3.74 (d, J = 5.1 Hz, 2 H), 3.40 (s, 6 H).

(3,4-Dimethoxybenzyl)(2,2-dimethoxyethyl)amine (8). The imine **7** (12.01 g, 47.47 mmol) was dissolved in ethanol (200 mL), and $NaBH_4$ (3.61 g, 95.4 mmol) was added over 0.5 h while the reaction mixture was stirred at reflux. The reaction mixture was diluted with water (200 mL). The amine was extracted into chloroform (250 mL) and the extract washed with water (2 × 150 mL) and brine (150 mL), dried (Na_2SO_4), and concentrated to provide a clear colorless oil (10.65 g, 88%). ^{1}H NMR (300 MHz, $CDCl_3$) δ 6.78−6.84 (m, 3 H), 4.44 (t, J = 5.4 Hz, 1 H), 3.88 (s, 3 H), 3.86 (s, 3 H), 3.70 (s, 2 H), 3.33 (s, 6 H), 2.69 (d, J = 5.4 Hz, 2 H).

2-Methylpiperonal (10). *n*-BuLi (2.5 M in THF, 26.4 mL, 66 mmol) was added dropwise to a solution of *N*,*N*,*N*′-(trimethyl)ethylenediamine (8.6 mL, 6.79 g, 66.4 mmol) in THF (120 mL) at −78 °C (acetone−dry ice bath). After 15 min, piperonal (9.0 g, 60 mmol) was added, the mixture was stirred for 15 min, and *n*-BuLi (2.5 M in THF, 72 mL, 180 mmol) was added via syringe. After the reaction mixture was stirred for 1 h at −78 °C, CH_3I (22.4 mL, 50.92 g, 360 mmol) was added at −78 °C. The mixture was stirred for 2 h at room temperature, poured into cold stirred 10% hydrochloric acid (prepared with 100 mL of concentrated hydrochloric acid and 360 mL of water), extracted with $CHCl_3$ (400 mL × 3), washed with brine (400 mL), dried (Na_2SO_4), filtered, and concentrated to give the crude product. Purification by preparative flash chromatography (SiO_2, EtOAc−hexane 10:1) gave the white crystalline product (6.71 g, 68.1%): mp 70−71 °C. ^{1}H NMR (300 MHz, $CDCl_3$) δ 9.96 (s, 1 H), 7.34 (d, J = 8.1 Hz, 1 H), 6.78 (d, J = 8.1 Hz, 1 H), 6.04 (s, 2 H), 2.50 (s, 3 H).

(*E*)-2-Methylpiperonal *O*-Methyloxime (11). 2-Methylpiperonal (**10**, 6.00 g, 36.5 mmol), *O*-methylhydroxyamine hydrochloride (6.11 g, 73.2 mmol), and sodium acetate hydrate (19.92 g, 146.4 mmol) were dissolved in methanol (200 mL), and the mixture was stirred at room temperature for 1 h. The reaction mixture was concentrated to dryness, ethyl acetate (200 mL) was added to the residue, and then 5% $NaHCO_3$ was added to neutralize acid. The solution was washed with brine (100 mL), dried (Na_2SO_4), filtered, and evaporated under vacuum to afford **11** (5.92 g, 84%) as a solid: mp 34 °C. IR (KBr) 2894, 1642, 1598, 1458, 1343, 1270, 1055 cm^{-1}; ^{1}H NMR (300 MHz, $CDCl_3$) δ 8.18 (s, 1 H), 7.17 (d, J = 8.1 Hz, 1 H), 6.66 (d, J = 8.1 Hz, 1 H), 5.96 (s, 2 H), 3.93 (s, 3 H), 2.28 (s, 3 H); low resolution ESIMS m/z (rel intensity) 194 (MH^+, 100). Anal. ($C_{10}H_{11}NO_3$) C, H, N.

(*E*)-2-Bromomethylpiperonal *O*-Methyloxime (12). A solution of the oxime **11** (4.00 g, 20.7 mmol), NBS (4.43 g, 2.49 mmol), and AIBN (0.4078 g, 2.49 mmol) in carbon tetrachloride (100 mL) was stirred at reflux under argon for 3 h. The reaction mixture was cooled to room temperature, filtered, and evaporated to give the crude product **12**. Purification by preparative flash chromatography (SiO_2, EtOAc−hexane 15:1) and then recrystallization from hexane gave the final pure product (3.27 g, 58%) as a white solid: mp 122−123 °C. IR (KBr) 2902, 1480, 1455, 1265, 1048, 927 cm^{-1}; ^{1}H NMR (300 MHz, $CDCl_3$) δ 8.19 (s, 1 H), 7.09 (d, J = 8.1 Hz, 1 H), 6.75 (d, J = 8.1 Hz, 1 H), 6.05 (s, 2 H), 4.73 (s, 2 H), 3.97 (s, 3 H); low resolution ESIMS m/z (rel intensity) 272 (MH^+, 37), 192 [$(M - Br)^+$, 100]. Anal. ($C_{10}H_{10}BrNO_3$) C, H, N.

(*E*)-4-[(Dimethylamino)methyl]benzo[*d*][1,3]dioxole-5-carbaldehyde *O*-Methyloxime (13a). A solution of the oxime **12** (0.40 g, 1.47 mmol) in THF (10 mL) was added by syringe during 15 min to dimethylamine (2 M in THF, 3 mL, 6 mmol) at 0 °C. The reaction mixture was stirred at room temperature for 2 h. The organic solvent was removed by evaporation under reduced pressure. A 5% $NaHCO_3$ aqueous solution (20 mL) was added to the residue, which was further extracted with EtOAc (40 mL × 2). The organic layer was washed with brine (5 mL) and dried (Na_2SO_4). Filtration and evaporation under reduced pressure gave **13a** as a yellow oil (0.3122 g, 90%). IR (KBr) 2939, 1474, 1455, 1253, 1053 cm^{-1}; ^{1}H NMR δ (300 MHz, $CDCl_3$) 8.39 (s, 1 H), 7.33(d, J = 8.1 Hz, 1 H), 6.73(d, J = 8.1 Hz, 1 H), 5.96 (s, 2 H), 3.93 (s, 3 H), 3.47 (s, 2 H), 2.22 (s, 6 H); low resolution ESIMS m/z (rel intensity) 237 (MH^+, 100), 192 [$(M-NHMe_2)^+$, 55]. Anal. ($C_{12}H_{16}N_2O_3$) C, H, N.

(*E*)-4-(Pyrrolidin-1-ylmethyl)benzo[*d*][1,3]dioxole-5-carbaldehyde *O*-Methyloxime (13b). A solution of the oxime **12** (0.95 g, 3.49 mmol) in THF (10 mL) was added by syringe to a solution of pyrrolidine (0.72 mL, 0.62 g, 8.7 mmol) in THF (10 mL) at 0 °C. The reaction mixture was stirred at room temperature for 2 h. The organic solvent was removed by evaporation under reduced pressure. An aqueous solution of 5% $NaHCO_3$ (20 mL) was added to the residue, and the mixture was extracted with EtOAc (40 mL × 2). The organic layer was washed with brine (20 mL) and dried (Na_2SO_4). Filtration and evaporation under reduced pressure gave **13b** as a yellow oil (0.801 g, 88%). IR (KBr) 2960, 1473, 1455, 1253, 1051 cm^{-1}; ^{1}H NMR (300 MHz, $CDCl_3$) δ 8.48 (s, 1 H), 7.35 (d, J = 8.1 Hz, 1 H), 6.74 (d, J = 8.1 Hz, 1 H), 5.97 (s, 2 H), 3.95 (s, 3 H), 3.70 (s, 2 H), 2.54 (broad s, 4 H), 1.72 (broad s, 4 H); ESIMS m/z (rel intensity) 263 (MH^+, 100). Anal. ($C_{14}H_{18}N_2O_3$) C, H, N.

(*E*)-4-[(1*H*-Imidazol-1-yl)methyl]benzo[*d*][1,3]dioxole-5-carbaldehyde *O*-Methyloxime (13c). A THF solution (3 mL) of the oxime **12** (0.40 g, 1.47 mmol) was added by syringe during 15 min to a solution of imidazole (0.40 g, 5.88 mmol) in THF (10 mL) at 0 °C. The reaction mixture was stirred at room temperature for 2 h. The organic solvent was removed by evaporation under reduced pressure. An aqueous 5% $NaHCO_3$ solution (10 mL) was added to the residue, and the mixture was extracted with EtOAc (40 mL × 2). The organic layer was washed with brine (20 mL) and dried (Na_2SO_4). Filtration and evaporation under reduced pressure gave **13c** as a yellow solid (0.32 g, 84%): mp 102 °C. IR (KBr) 2964, 1462, 1271, 1051 cm^{-1}; ^{1}H NMR (300 MHz, $CDCl_3$) δ 8.06 (s, 1 H), 7.63 (s, 1 H), 7.03 (brs, 1 H), 6.97 (brs, 1 H), 6.90 (d, J = 8.1 Hz, 1 H), 6.78 (d, J = 8.1 Hz, 1 H), 6.04 (s, 2 H), 5.43 (s, 2 H), 3.96 (s, 3 H); ESIMS m/z (rel intensity) 260 (MH^+, 100). Anal. ($C_{13}H_{13}N_3O_3$) C, H, N.

4-[(4-Methylpiperazin-1-yl)methyl]benzo[*d*][1,3]dioxole-5-carbaldehyde *O*-Methyloxime (13d). A solution of the oxime **12** (360.0 mg, 1.324 mmol) in THF (10 mL) was added by syringe during 30 min to a solution of 4-methylpiperazine (400.0 mg, 4.00 mmol) in THF (10 mL) at 0 °C. The reaction mixture was then stirred at room temperature for 4 h. The organic solvent was removed by evaporation under reduced pressure. An aqueous 5% $NaHCO_3$ solution (20 mL) was added to the residue, and the mixture was extracted with EtOAc (40 mL × 2). The organic layer was washed with brine (20 mL) and dried (Na_2SO_4).

Filtration and evaporation under reduced pressure gave **13d** as a yellow solid (303.1 mg, 78%): mp 100−102 °C. IR 2937, 1473, 1455, 1295, 1050 cm^{-1}; ^1H NMR (300 MHz, $CDCl_3$) δ 8.47 (s, 1 H), 7.39 (d, J = 8.2 Hz, 1 H), 6.74 (d, J = 8.2 Hz, 1 H), 5.97 (s, 2 H), 3.96 (s, 3 H), 3.96 (s, 2 H), 3.53 (s, 3 H), 2.46 (brs, 8 H), 2.26 (s, 3 H); ESIMS m/z (rel intensity) 292 (MH^+, 100), 192 (10).

4-(Morpholinomethyl)benzo[*d*][1,3]dioxole-5-carbaldehyde *O*-Methyloxime (13e). A solution of the oxime **12** (400.0 mg, 1.47 mmol) in THF (10 mL) was added by syringe during 30 min to a solution of morpholine (510.0 mg, 5.86 mmol) in THF (10 mL) at 0 °C. The reaction mixture was stirred at room temperature for 2 h. The organic solvent was removed by evaporation under reduced pressure. An aqueous 5% $NaHCO_3$ solution (20 mL) was added to the residue, and the mixture was extracted with EtOAc (40 mL × 2). The organic layer was washed with brine (20 mL) and dried (Na_2SO_4). Filtration and evaporation under reduced pressure gave **13e** as a yellow oil (369.0 mg, 90.2%). IR 2896, 1473, 1455, 1254, 1050 cm^{-1}; ^1H NMR (300 MHz, $CDCl_3$) δ 8.46 (s, 1 H), 7.38 (d, J = 8.4 Hz, 1 H), 6.74 (d, J = 8.4 Hz, 1 H), 5.98 (s, 2 H), 3.95 (s, 3 H), 3.67 (t, J = 4.6 Hz, 4 H), 3.53 (s, 2 H), 2.44 (t, J = 4.6 Hz, 4 H); ESIMS m/z (rel intensity) 279 (MH^+, 100), 192 (30).

4-(((2-(Dimethylamino)ethyl)(methyl)amino)methyl)benzo[*d*]-[1,3]dioxole-5-carbaldehyde *O*-Methyloxime (13f). A solution of the oxime **12** (908.1 mg, 3.34 mmol) in THF (10 mL) was added by syringe during 15 min to *N*,*N*,*N*′-trimethylethylenediamine (1021.2 mg, 9.994 mmol) in THF (5 mL) at 0 °C. The reaction mixture was stirred at room temperature for 4 h. The organic solvent was removed by evaporation under reduced pressure. An aqueous 5% $NaHCO_3$ solution (10 mL) was added to the residue, which was further extracted with EtOAc (20 mL × 2). The organic layer was washed with brine (10 mL) and dried (Na_2SO_4). Filtration and evaporation under reduced pressure gave **13f** as a yellow oil (485.2 mg, 49.4%). IR 2939, 1473, 1455, 1254, 1051 cm^{-1}; ^1H NMR (300 MHz, $CDCl_3$) δ 8.51 (s, 1 H), 7.37 (d, J = 8.1 Hz, 1 H), 6.73 (d, J = 8.1 Hz, 1 H), 5.97 (s, 2 H), 3.94 (s, 3 H), 3.59 (s, 3 H), 2.52 (t, J = 6.5 Hz, 2 H), 2.43 (t, J = 6.5 Hz, 2 H), 2.21 (s, 9 H); ESIMS m/z (rel intensity) 294 (MH^+, 100), 249 [$(M - Me_2NH)^+$, 80].

2,3-Dimethoxy-8,9-methylenedioxy-10-(dimethylamino)methyl-11*H*-indeno[1,2-*c*]isoquinoline (14a). The amine **8** (0.30 g, 1.18 mmol) and oxime ether **13a** (0.126 g, 0.534 mmol) were mixed with concentrated hydrochloric acid (7 mL), and the mixture was stirred at 100 °C for 18 h. The reaction mixture was cooled and washed with ether (3 × 20 mL). It was then brought to basic pH with NH_4OH. The mixture was extracted with chloroform (40 mL × 3), and the solution was washed with brine (50 mL), dried (Na_2SO_4), and concentrated. The residue was diluted in chloroform (40 mL) and filtered. Hydrochloric acid (2 M HCl in ether, 5 mL) was added to the filtrate. The precipitate that formed was recrystallized from methanol to provide a yellow solid. The solid was dissolved in water, basified with NH_4OH, and extracted with chloroform. The organic layer was concentrated to dryness. The residue was purified by preparative flash chromatography (SiO_2, methanol−chloroform−TEA = 3:97:2) to afford the final product **14a** as a light-yellow solid (0.0162 g, 7.8%): mp 205−207 °C. IR (KBr) 2940, 1449, 1408, 1326, 1246, 1159, 1061 cm^{-1}; ^1H NMR (300 MHz, $CDCl_3$) δ 8.98 (s, 1 H), 7.62 (s, 1 H), 7.23 (s, 1 H), 7.16 (s, 1 H), 6.11 (s, 2 H), 4.21 (s, 2 H), 4.10 (s, 3 H), 4.05 (s, 3 H), 2.77 (s, 6 H); low resolution ESIMS m/z (rel intensity) 379 (MH^+, 100), 334 (90). Anal. ($C_{22}H_{22}N_2O_4 \cdot 1.25H_2O$) C, H, N.

2,3-Dimethoxy-8,9-methylenedioxy-10-(pyrrolidin-1-yl)methyl-11*H*-indeno[1,2-*c*]isoquinoline (14b). The amine **8** (1.90 g, 7.45 mmol) and oxime ether **13b** (0.90 g, 3.44 mmol) were mixed with concentrated hydrochloric acid (15 mL), and the mixture was stirred at 100 °C for 18 h. The reaction mixture was then cooled and washed with ether (3 × 20 mL). It was then brought to basic pH with NH_4OH. The mixture was extracted with chloroform (40 mL × 3), and the solution was washed with brine (50 mL), dried (Na_2SO_4), and concentrated. The residue was dissolved in chloroform (40 mL) and filtered. Hydrochloric acid (2 M HCl in ether, 5 mL) was added to the filtrate. The precipitate that formed was recrystallized from methanol to provide a yellow solid. The solid was dissolved in water, basified with NH_4OH, and extracted with chloroform. The organic layer was concentrated to dryness. The residue was purified by preparative flash chromatography (SiO_2, methanol−chloroform−TEA = 3:97:2) to yield the final pure product **14b** as a light-yellow solid (84.9 mg, 6.1%): mp 210 °C (dec). IR (KBr) 2958, 1449, 1406, 1326, 1246 cm^{-1}; ^1H NMR (300 MHz, $CDCl_3$) δ 8.94 (s, 1 H), 7.44 (s, 1 H), 7.16 (s, 1 H), 7.01 (s, 1 H), 6.04 (s, 2 H), 4.07 (s, 3 H), 4.02 (s, 3 H), 3.85 (s, 2 H), 3.79 (s, 2 H), 2.67 (broad s, 4 H), 1.82 (broad s, 4 H); low resolution ESIMS m/z (rel intensity) 405 (MH^+, 15), 334 (100). Anal. ($C_{24}H_{24}N_2O_4 \cdot 1.75H_2O$) C, H, N.

2,3-Dimethoxy-8,9-methylenedioxy-10-(1*H*-imidazol-yl)methyl-11*H*-indeno[1,2-*c*]isoquinoline (14c). The amine **8** (0.905 g, 3.55 mmol) and oxime ether **13c** (0.41 g, 1.6 mmol) were mixed with concentrated hydrochloric acid (8 mL), and the mixture was stirred at 100 °C for 18 h. The reaction mixture was then cooled and washed with ether (3 × 20 mL). It was then brought to basic pH with NH_4OH. The mixture was extracted with chloroform (40 mL × 3), and the solution was washed with brine (50 mL), dried (Na_2SO_4), and concentrated. The residue was diluted in chloroform (40 mL) and filtered. Hydrochloric acid (2 M HCl in ether, 5 mL) was added to the filtrate. The precipitate that formed was recrystallized from methanol to provide a yellow solid. The solid was dissolved in water, basified with NH_4OH, and extracted with chloroform. The organic layer was concentrated to dryness. The residue was purified by preparative flash chromatography (SiO_2, methanol−chloroform−TEA = 10:90:2) to afford the final pure product **14c** as a light-brown solid (0.0419 g, 6.6%): mp 250 °C (dec). IR (KBr) 2961, 1496, 1413, 1207, 1020 cm^{-1}; ^1H NMR (300 MHz, DMSO) δ 9.01 (s, 1 H), 7.84 (s, 1 H), 7.54 (s, 1 H), 7.39 (s, 1 H), 7.31 (s, 1 H), 7.24 (s, 1 H), 6.90 (s, 1 H), 6.15 (s, 2 H), 5.33 (s, 2 H), 4.08 (s, 2 H), 3.99 (s, 3 H), 3.92 (s, 3 H); low resolution ESIMS m/z (rel intensity) 402 (MH^+, 100), 334 (15). Anal. ($C_{23}H_{19}N_3O_4 \cdot 1.5H_2O$) C, H, N.

2,3-Dimethoxy-8,9-methylenedioxy-10-(4-methylpiperazin-1-yl)-methyl-11*H*-indeno[1, 2-*c*]isoquinoline (14d). The amine **8** (560.3 mg, 2.19 mmol) and oxime ether **13d** (320.2 mg, 1.10 mmol) were mixed together with concentrated hydrochloric acid (10 mL), and the mixture was stirred at 100 °C for 3 h. The reaction mixture was then cooled and washed with ether (3 × 20 mL). It was then brought to basic pH with 28% aqueous NH_4OH. The mixture was extracted with $CHCl_3$ (3 × 40 mL), and the organic layer was washed with brine (50 mL), dried with anhydrous Na_2SO_4, and concentrated. The residue was diluted in $CHCl_3$ (40 mL) and filtered. Hydrochloric acid (2 M HCl in ether, 10 mL) was added to the filtrate. A dark-yellow precipitate was obtained and recrystallized from methanol to provide a bright-yellow solid. NH_4OH (2 mL) was added to the yellow solid, and the mixture was concentrated to dryness. The residue was purified by preparative flash chromatography (SiO_2, methanol−chloroform−TEA = 10:90:2) to yield the final pure product **14d** as a yellow solid (16.7 mg, 3.5%): mp 296 °C (dec). IR 3400, 1489, 1455, 1245, 1159 cm^{-1}; ^1H NMR (300 MHz, $CDCl_3$) δ 8.98 (s, 1 H), 7.47 (s, 1 H), 7.24 (s, 1 H), 7.08 (s,1 H), 6.04 (s, 2 H), 4.11 (s, 3 H), 4.04 (s, 3 H), 3.91 (s, 2 H), 3.68 (s, 2 H), 2.65 (brs, 4 H), 2.56 (brs, 4 H), 2.34 (s, 3 H); ESIMS m/z (rel intensity) 434 (MH^+, 100), 334 (25). Anal. ($C_{25}H_{27}N_3O_4 \cdot 3.5H_2O$) C, H, N.

2,3-Dimethoxy-8,9-methylenedioxy-10-(4-morpholino)methyl-11*H*-indeno[1,2-*c*]isoquinoline (14e). The amine **8** (660.0 mg, 2.59 mmol) and oxime **13e** (320.0 mg, 1.15 mmol) were mixed together with concentrated hydrochloric acid (10 mL) and stirred at 100 °C for 3 h. The reaction mixture was cooled and washed with ether (3 × 20 mL). It was brought to basic pH with 28% aqueous NH_4OH. The mixture was extracted with $CHCl_3$ (3 × 40 mL), and the organic layer was washed with brine (50 mL), dried with anhydrous Na_2SO_4, and concentrated. The residue

was diluted in $CHCl_3$ (40 mL) and filtered. Hydrochloric acid (2 M HCl in ether, 10 mL) was added to the filtrate. A dark-yellow precipitate was obtained and then recrystallized from methanol to provide a bright-yellow solid. NH_4OH (2 mL) was added to the yellow solid, and the mixture was extracted with $CHCl_3$ (3×20 mL) and concentrated to dryness. The residue was purified by preparative flash chromatography (SiO_2, methanol−chloroform−TEA = 5:95:2) to afford the final pure product as a golden crystalline solid **14e** (32.2 mg, 6.7%): mp 269 °C (dec). IR 3400, 1489, 1455, 1249, 1115 cm^{-1}; ^1H NMR (300 MHz, $CDCl_3$) δ 8.99 (s, 1 H), 7.49 (s, 1 H), 7.11 (s, 1 H), 6.04 (s, 2 H), 4.12 (s, 3 H), 4.05 (s, 3 H), 3.97 (s, 2 H), 3.72 (t, $J = 4.5$ Hz, 4 H), 3.68 (s, 2 H), 2.56 (t, $J = 4.5$ Hz, 4 H); ESIMS m/z (rel intensity) 421 (MH^+, 100), 334 (32). Anal. ($C_{24}H_{24}N_2O_5 \cdot 0.4H_2O$) C, H, N.

2,3-Dimethoxy-8,9-methylenedioxy-10-(*N*,*N*,*N*′-trimethylethylenediamino)methyl-11*H*-indeno[1,2-*c*]isoquinoline (14f). The amine **8** (1020 mg, 4.00 mmol) and oxime ether **13f** (458.1 mg, 1.56 mmol) were mixed together with concentrated hydrochloric acid (10 mL), and the mixture was stirred at 100 °C for 18 h. The reaction mixture was cooled and washed with ether (3×20 mL). It was then brought to basic pH with NaOH (10% aqueous) at 0 °C (water−ice bath). The mixture was extracted with $CHCl_3$ (3×40 mL), and the organic layer was washed with brine (50 mL), dried with anhydrous Na_2SO_4, and concentrated. The residue was diluted in $CHCl_3$ (40 mL) and filtered. Hydrochloric acid (2 M HCl in ether, 10 mL) was added to the filtrate. The dark-yellow precipitate was recrystallized from methanol to provide a bright-yellow solid. NH_4OH (2 mL) was added to the yellow solid, and the mixture was concentrated to dryness. The residue was purified by preparative flash chromatography (SiO_2, methanol−chloroform−TEA = 10:90:2) to provide the final pure product as a yellow solid **14f** (21.1 mg, 3.1%): mp 192 °C. IR 3400, 2944, 1488, 1247, 1060 cm^{-1}; ^1H NMR (300 MHz, $CDCl_3$) δ 8.95 (s, 1 H), 7.45 (s, 1 H), 7.20 (s, 1 H), 7.04 (s, 1 H), 6.03 (s, 2 H), 4.09 (s, 3 H), 3.91 (s, 3 H), 3.84 (s, 2 H), 3.62 (s, 2 H), 2.58 (t, $J = 6.3$ Hz, 2 H), 2.50 (t, $J = 6.3$ Hz, 2 H), 2.29 (s, 3 H), 2.22 (s, 6 H); ESIMS m/z (rel intensity) 436 (MH^+, 85), 391($MH^+ - Me_2NH$, 22), 334 ($MH^+ - CH_3NHCH_2CH_2N(CH_3)_2$, 100); HRESIMS calculated 435.2236, found 436.2240 (MH^+); purity 98.6% (HPLC).

2,3-Dimethoxy-8,9-methylenedioxy-10-methyl-11*H*-indeno[1,2-*c*]isoquinoline (15). The amine **8** (0.640 g, 2.51 mmol) and 2-methylpiperonal (**10**, 0.450 g, 2.74 mmol) were mixed with concentrated hydrochloric acid (8 mL), and the mixture was stirred at 100 °C for 18 h. The reaction mixture was then cooled and washed with ether (3×20 mL). It was then brought to basic pH with NH_4OH. The mixture was extracted with chloroform (40 mL × 3), and the solution was washed with brine (50 mL), dried (Na_2SO_4), and concentrated. The residue was dissolved in chloroform (40 mL) and filtered. Hydrochloric acid (2 M HCl in ether, 8.7 mL) was added to the filtrate. The precipitate that formed was recrystallized from methanol to provide a yellow solid. The solid was dissolved in water, basified with NH_4OH, and extracted with chloroform. The organic layer was concentrated to dryness. The residue was purified by preparative flash chromatography (SiO_2, acetone−chloroform−TEA = 20:80:2) to afford the final pure product as a light-yellow solid (0.025 g, 3.0%): mp 272−274 °C (dec). IR (KBr) 2902, 1487, 1240, 1075 cm^{-1}; ^1H NMR (300 MHz, $CDCl_3$) δ 8.96 (s, 1 H), 7.41 (s, 1 H), 7.22 (s, 1 H), 7.21 (s, 1 H), 6.02 (s, 2 H), 4.07 (s, 3 H), 4.02 (s, 3 H), 3.78 (s, 2 H), 2.33 (s, 3 H); low resolution ESIMS m/z (rel intensity) 336 (MH^+, 100). Anal. ($C_{20}H_{17}NO_4 \cdot 0.5H_2O$) C, H, N.

Topoisomerase I Mediated DNA Cleavage Reactions. Human recombinant Top1 was purified from baculovirus as previously described.[46] DNA cleavage reactions were prepared as previously reported with the exception of the DNA substrate.[13] Briefly, a 117-bp DNA oligonucleotide (Integrated DNA Technologies) encompassing the previously identified Top1 cleavage sites in the 161-bp fragment from pBluescript SK(−) phagemid DNA was employed. This 117-bp oligonucleotide contains a single 5′-cytosine overhang, which was 3′-end-labeled by fill-in reaction with [α-^{32}P]dGTP in React 2 buffer (50 mM Tris-HCl, pH 8.0, 100 mM $MgCl_2$, 50 mM NaCl) with 0.5 units of DNA polymerase I (Klenow fragment, New England BioLabs). Unincorporated [^{32}P]dGTP was removed using mini Quick Spin DNA columns (Roche, Indianapolis, IN), and the eluate containing the 3′-end-labeled DNA substrate was collected. Approximately 2 nM of radiolabeled DNA substrate was incubated with recombinant Top1 in 20 μL of reaction buffer [10 mM Tris-HCl (pH 7.5), 50 mM KCl, 5 mM $MgCl_2$, 0.1 mM EDTA, and 15 μg/mL BSA] at 25 °C for 20 min in the presence of various concentrations of compounds. The reactions were terminated by adding SDS (0.5% final concentration) followed by the addition of two volumes of loading dye (80% formamide, 10 mM sodium hydroxide, 1 mM sodium EDTA, 0.1% xylene cyanol, and 0.1% bromphenol blue). Aliquots of each reaction mixture were subjected to 20% denaturing PAGE. Gels were dried and visualized by using a phosphoimager and ImageQuant software (Molecular Dynamics). For simplicity, cleavage sites were numbered as previously described in the 161-bp fragment.[47]

Molecular Docking. Norindenoisoquinoline **14b** was built on the basis of the crystal structure of **14a** in the SYBYL 8.0.3 software from Tripos.[48] The protonated form of **14b** was further built by modifying the atom type of the pyrrolidine nitrogen atom from N3 to N4 and then adding hydrogen atoms. Both molecules were minimized using the MMFF94s force field, MMFF94 charges, and the conjugate gradient method, with simplex initial optimization, to a gradient of less than 0.001 kcal/mol. The conformations were docked to Top1−DNA complex (PDB code 1tl8) by CCDC's molecular docking software GOLD[49] 3.0.1 using default settings. The binding region was defined as all the atoms that are 12 Å around the centroid of norindenoisoquinoline **5** in the crystal structure. Early termination was allowed if the top three solutions were within 1.5 Å rms deviation. To rank docking results, the GoldScore fitness scores were used. The top three energy-ranked structures for each ligand were saved for graphic analysis. The resulting complexes were further minimized using MMFF94s force field, MMFF94 charges as above. The binding energies were calculated by the following equation:

$$E_{\text{binding}} = E_{\text{complex}} - E_{\text{protein}} - E_{\text{ligand}}$$

Quantum Chemistry Calculation. The DNA-binding energies of **14a** and **15** to the simplified DNA cleavage site of Top1, and the solvation energies, were calculated using the methods and strategies described in detail in our earlier publication.[37] First, the molecules were built starting from the crystal structure of **14a** in SYBYL and geometry optimizations and frequency calculations were carried out for each compound at the HF/6-31G** level. The energy-minimized structures displayed no imaginary frequencies and were therefore utilized to replace the original ligand in the simplified DNA model. The model was then subjected to single-point energy calculations using the MP2 method at the modified 6-31G*(0.25) level using the quantum chemical program package Gaussian 03.[50] The effect of solvation was investigated using the polarizable continuum model (PCM) at the MP2/6-31G*(0.25) level with the default radii scheme.

The intermolecular interaction energy was calculated using the supermolecular approach. The energy of interaction between the ligand and the neighboring DNA base pairs is defined as the difference between the energy of the complex E_{complex} and the energies of the monomers E_{ligand} and E_{bp}. The basis set superposition error (BSSE) was also corrected using the Boys and Bernardi counterpoise method because of the use of an incomplete basis set in practical applications of the supermolecular approach. Therefore, the interaction energies of the two

compounds **14a** and **15** were calculated at the MP2/6-31G*(0.25) level through the following equation:

$$E_{int} = E_{complex} - E_{ligand} - E_{bp} + BSSE$$

Acknowledgment. This work was made possible by the National Institutes of Health (NIH) through support of this work with Research Grant UO1 CA89566. Some of this research was conducted in a facility constructed with the financial support of a Research Facilities Improvement Program Grant C06-14499 from the National Institutes of Health. We thank the Rosen Center for Advanced Computing (RCAC), Purdue University, for providing computing facilities.

Supporting Information Available: Elemental analysis results for compounds **11**, **12**, **13a**−**c**, **14a**−**e**, and **15**; HPLC trace for compound **14f**; docking scores; binding energies; and calculated physical chemical properties including log *P*, log *D*, pK_a. This material is available free of charge via the Internet at http://pubs.acs.org.

References

(1) Pommier, E. Topoisomerase I Inhibitors: Camptothecins and Beyond. *Nat. Rev. Cancer* **2006**, *6*, 789–802.
(2) Champoux, J. J. DNA Topoisomerases: Structure, Function, and Mechanism. *Annu. Rev. Biochem.* **2001**, *70*, 369–413.
(3) Kehrer, D. F. S.; Soepenberg, O.; Loos, W.; Verweij, J.; Sparreboom, A. Modulation of Camptothecin Analogs in the Treatment of Cancer: A Review. *Anti-Cancer Drugs* **2001**, *12*, 89–105.
(4) Garcia-Carbonero, R.; Supko, J. G. Current Perspectives on the Clinical Experience, Pharmacology, and Continued Development of the Camptothecins. *Clin. Cancer Res.* **2002**, *8*, 641–661.
(5) Scott, D. O.; Bindra, D. S.; Stella, V. J. Plasma Pharmacokinetics of the Lactone and Carboxylate Forms of 20(*S*)-Camptothecin in Anesthetized Rats. *Pharm. Res.* **1993**, *10*, 1451–1457.
(6) Burke, T. G.; Mi, Z. H. The Structural Basis of Camptothecin Interactions with Human Serum-Albumin. Impact on Drug Stability. *J. Med. Chem.* **1994**, *37*, 40–46.
(7) Hsiang, Y. H.; Liu, L. F. Identification of Mammalian DNA Topoisomerase-I as an Intracellular Target of the Anticancer Drug Camptothecin. *Cancer Res.* **1988**, *48*, 1722–1726.
(8) Fujimori, A.; Harker, W. G.; Kohlhagen, G.; Hoki, Y.; Pommier, Y. Mutation at the Catalytic Site of Topoisomerase I in CEM/C2, a Human Leukemia Cell Resistant to Camptothecin. *Cancer Res.* **1995**, *55*, 1339–1346.
(9) Urasaki, Y.; Laco, G. S.; Pourquier, P.; Takebayashi, Y.; Kohlhagen, G.; Gioffre, C.; Zhang, H. L.; Chatterjee, D.; Pantazis, P.; Pommier, Y. Characterization of a Novel Topoisomerase I Mutation from a Camptothecin-Resistant Human Prostate Cancer Cell Line. *Cancer Res.* **2001**, *61*, 1964–1969.
(10) Nakagawa, H.; Saito, H.; Ikegami, Y.; Aida-Hyugaji, S.; Seigo, S.; Ishikawa, T. Molecular Modeling of New Camptothecin Analogues To Circumvent ABCG2-Mediated Drug Resistance in Cancer. *Cancer Lett.* **2006**, *234*, 81–89.
(11) Pommier, Y.; Pourquier, P.; Fan, Y.; Strumberg, D. Mechanism of Action of Eukaryotic DNA Topoisomerases and Drugs Targeted to the Enzyme. *Biochem. Biophys. Acta* **1998**, *1400*, 83–105.
(12) Gottlieb, J. A.; Luce, J. K. Treatment of Malignant Melanoma with Camptothecin (NSC-100880). *Cancer Chemother. Rep.* **1972**, *56*, 103–105.
(13) Dexheimer, T. S.; Pommier, Y. DNA Cleavage Assay for the Identification of Topoisomerase I Inhibitors. *Nat. Protoc.* **2008**, *3*, 1736–1750.
(14) Li, Q.-Y.; Zu, Y.-G.; Shi, R.-Z.; Yao, L.-P. Review of Camptothecin: Current Perspectives. *Curr. Med. Chem.* **2006**, *13*, 2021–2039.
(15) Teicher, B. Next Generation of Topoisomerase I Inhibitors: Rationale and Biomarker Strategies. *Biochem. Pharmacol.* **2008**, *75*, 1262–1271.
(16) Pommier, Y. DNA Topoisomerase I Inhibitors: Chemistry, Biology, and Interfacial Inhibition. *Chem. Rev.* **2009**, *109*, 2894–2902.
(17) Pommier, Y.; Cushman, M. The Indenoisoquinoline Noncamptothecin Topoisomerase I Inhibitors: Update and Perspectives. *Mol. Cancer Ther.* **2009**, *8*, 1008–1014.
(18) Yamada, Y.; Tamura, T.; Yamamoto, N.; Shimoyama, T.; Ueda, Y.; Murakami, H.; Kusaba, H.; Kamiya, Y.; Saka, H.; Tanigawara, Y.; McGovren, J. P.; Natsumeda, Y. Phase I and Pharmacokinetic Study of Edotecarin, a Novel Topoisomerase I Inhibitor, Administered Once Every 3 Weeks in Patients with Solid Tumors. *Cancer Chemother. Pharmacol.* **2006**, *58*, 173–182.
(19) Kohlhagen, G.; Paull, K.; Cushman, M.; Nagafuji, P.; Pommier, Y. Protein-Linked DNA Strand Breaks Induced by NSC 314622, a Novel Noncamptothecin Topoisomerase I Poison. *Mol. Pharmacol.* **1998**, *54*, 50–58.
(20) Cushman, M.; Jayaraman, M.; Vroman, J. A.; Fukunaga, A. K.; Fox, B. M.; Kohlhagen, G.; Strumberg, D.; Pommier, Y. Synthesis of New Indeno[1,2-*c*]isoquinolines: Cytotoxic Non-Camptothecin Topoisomerase I Inhibitors. *J. Med. Chem.* **2000**, *43*, 3688–3698.
(21) Fox, B. M.; Xiao, X.; Antony, S.; Kohlhagen, G.; Pommier, Y.; Staker, B. L.; Stewart, L.; Cushman, M. Design, Synthesis, and Biological Evaluation of Cytotoxic 11-Alkenylindenoisoquinoline Topoisomerase I Inhibitors and Indenoisoquinoline−Camptothecin Hybrids. *J. Med. Chem.* **2003**, *46*, 3275–3282.
(22) Morrell, A.; Antony, S.; Kohlhagen, G.; Pommier, Y.; Cushman, M. Synthesis of Nitrated Indenoisoquinolines as Topoisomerase I Inhibitors. *Bioorg. Med. Chem. Lett.* **2004**, *14*, 3659–3663.
(23) Morrell, A.; Antony, S.; Kohlhagen, G.; Pommier, Y.; Cushman, M. A Systematic Study of Nitrated Indenoisoquinolines Reveals a Potent Topoisomerase I Inhibitor. *J. Med. Chem.* **2006**, *49*, 7740–7753.
(24) Morrell, A.; Antony, S.; Kohlhagen, G.; Pommier, Y.; Cushman, M. Synthesis of Benz[*d*]indeno[1,2-*b*]pyran-5,11-diones: Versatile Intermediates for the Design and Synthesis of Topoisomerase I Inhibitors. *Bioorg. Med. Chem. Lett.* **2006**, *16*, 1846–1849.
(25) Morrell, A.; Jayaraman, M.; Nagarajan, M.; Fox, B. M.; Meckley, M. R.; Ioanoviciu, A.; Pommier, Y.; Antony, S.; Hollineshead, M.; Cushman, M. Evaluation of Indenoisoquinoline Topoisomerase I Inhibitors Using a Hollow Fiber Assay. *Bioorg. Med. Chem. Lett.* **2006**, *16*, 4395–4399.
(26) Morrell, A.; Placzek, M.; Parmley, S.; Antony, S.; Dexheimer, T. S.; Pommier, Y.; Cushman, M. Nitrated Indenoisoquinolines as Topoisomerase I Inhibitors: A Systematic Study and Optimization. *J. Med. Chem.* **2007**, *50*, 4419–4430.
(27) Morrell, A.; Placzek, M.; Parmley, S.; Grella, B.; Antony, S.; Pommier, Y.; Cushman, M. Optimization of the Indenone Ring of Indenoisoquinoline Topoisomerase I Inhibitors. *J. Med. Chem.* **2007**, *50*, 4388–4404.
(28) Morrell, A.; Placzek, M. S.; Steffen, J. D.; Antony, S.; Agama, K.; Pommier, Y.; Cushman, M. Investigation of the Lactam Side Chain Length Necessary for Optimal Indenoisoquinoline Topoisomerase I Inhibition and Cytotoxicity in Human Cancer Cell Cultures. *J. Med. Chem.* **2007**, *50*, 2040–2048.
(29) Nagarajan, M.; Morrell, A.; Antony, S.; Kohlhagen, G.; Agama, K.; Pommier, Y.; Ragazzon, P. A.; Garbett, N. C.; Chaires, J. B.; Hollingshead, M.; Cushman, M. Synthesis and Biological Evaluation of Bisindenoisoquinolines as Topoisomerase I Inhibitors. *J. Med. Chem.* **2006**, *49*, 5129–5140.
(30) Nagarajan, M.; Morrell, A.; Fort, B. C.; Meckley, M. R.; Antony, S.; Kohlhagen, G.; Pommier, Y.; Cushman, M. Synthesis and Anticancer Activity of Simplified Indenoisoquinoline Topoisomerase I Inhibitors Lacking Substituents on the Aromatic Rings. *J. Med. Chem.* **2004**, *47*, 5651–5661.
(31) Nagarajan, M.; Morrell, A.; Ioanoviciu, A.; Antony, S.; Kohlhagen, G.; Agama, K.; Hollingshead, M.; Pommier, Y.; Cushman, M. Synthesis and Evaluation of Indenoisoquinoline Topoisomerase I Inhibitors Substituted with Nitrogen Heterocycles. *J. Med. Chem.* **2006**, *49*, 6283–6289.
(32) Nagarajan, M.; Xiao, X.; Antony, S.; Kohlhagen, G.; Pommier, Y.; Cushman, M. Design, Synthesis, and Biological Evaluation of Indenoisoquinoline Topoisomerase I Inhibitors Featuring Polyamine Side Chains on the Lactam Nitrogen. *J. Med. Chem.* **2003**, *46*, 5712–5724.
(33) Strumberg, D.; Pommier, Y.; Paull, K.; Jayaraman, M.; Nagafuji, P.; Cushman, M. Synthesis of Cytotoxic Indenoisoquinoline Topoisomerase I Poisons. *J. Med. Chem.* **1999**, *42*, 446–457.
(34) Antony, S.; Agama, K. K.; Miao, Z. H.; Takagi, K.; Wright, M. H.; Robles, A. I.; Varticovski, L.; Nagarajan, M.; Morrell, A.; Cushman, M.; Pommier, Y. Novel Indenoisoquinolines NSC 725776 and NSC 724998 Produce Persistent Topolsomerase I Cleavage Complexes and Overcome Multidrug Resistance. *Cancer Res.* **2007**, *67*, 10397–10405.
(35) Ioanoviciu, A.; Antony, S.; Pommier, Y.; Staker, B. L.; Stewart, L.; Cushman, M. Synthesis and Mechanism of Action Studies of a Series of Norindenoisoquinoline Topoisomerase I Poisons Reveal an Inhibitor with a Flipped Orientation in the Ternary DNA−Enzyme−Inhibitor Complex As Determined by X-ray Crystallographic Analysis. *J. Med. Chem.* **2005**, *48*, 4803–4814.
(36) Marchand, C.; Antony, S.; Kohn, K. W.; Cushman, M.; Ioanoviciu, A.; Staker, B. L.; Burgin, A.; Stewart, L.; Pommier, Y. A Novel

Norindenoisoquinoline Structure Reveals a Common Interfacial Inhibitor Paradigm for Ternary Trapping of the Topoisomerase I−DNA Complex. *Mol. Cancer Ther.* **2006**, *5*, 287–295.
(37) Song, Y. L.; Cushman, M. The Binding Orientation of a Norindenoisoquinoline in the Topoisomerase I−DNA Cleavage Complex Is Primarily Foverned by pi−pi Stacking Interactions. *J. Phys. Chem. B* **2008**, *112*, 9484–9489.
(38) Staker, B. L.; Feese, M. D.; Cushman, M.; Pommier, Y.; Zembower, D.; Stewart, L.; Burgin, A. B. Structures of Three Classes of Anticancer Agents Bound to the Human Topoisomerase I−DNA Covalent Complex. *J. Med. Chem.* **2005**, *48*, 2336–2345.
(39) Staker, B. L.; Hjerrild, K.; Feese, M. D.; Behnke, C. A.; Burgin, A. B.; Stewart, L. The Mechanism of Topoisomerase I Poisoning by a Camptothecin Analogue. *Proc. Natl. Acad. Sci. U.S.A.* **2002**, *99*, 15387–15392.
(40) Carrigan, S. W.; Fox, P. C.; Wall, M. E.; Wani, M. C.; Bowen, J. P. Comparative Molecular Field Analysis and Molecular Modeling Studies of 20-(*S*)-Camptothecin Analogs as Inhibitors of DNA Topoisomerase I and Anticancer/Antitumor Agents. *J. Comput. Aided Mol. Des.* **1997**, *11*, 71–78.
(41) Gensler, W. J. The Synthesis of Isoquinolines by the Pomeranz−Fritsch Reaction. *Org. React.* **1951**, *6*, 191–206.
(42) Bobbitt, J. M.; Winter, D. P.; Kiely, J. M. Synthesis of Isoquinolines. IV. 4-Benzylisoquinolines. *J. Org. Chem.* **1965**, *30*, 2459–2460.
(43) Birch, A. J.; Jackson, A. H.; Shannon, P. V. R. New Modification of the Pomeranz−Fritsch Isoquinoline Synthesis. *J. Chem. Soc., Perkin Trans. 1* **1974**, 2185–2190.
(44) Comins, D. L.; Brown, J. D. Ortho Metalation Directed by Alpha-Amino Alkoxides. *J. Org. Chem.* **1984**, *49*, 1078–1083.
(45) Boyd, M. R.; Paull, K. D. Some Practical Considerations and Applications of the National Cancer Institute in Vitro Anticancer Drug Discovery Screen. *Drug Dev. Res.* **1995**, *34*, 91–109.
(46) Shoemaker, R. H. The NCI60 Human Tumour Cell Line Anticancer Drug screen. *Nat. Rev. Cancer* **2006**, *6*, 813–823.
(47) Balogh, G. T.; Gyarmati, B.; Nagy, B.; Molnár, L.; Keserü, G. M. Comparative Evaluation of in Silico pK_a Prediction Tools on the Gold Standard Dataset. *QSAR Comb. Sci.* **1009**, *28*, 1148–1155.
(48) *SYBYL*, version 8.0.3; Tripos: St. Louis, MO.
(49) *GOLD*, version 3.0.1; The Cambridge Crystallographic Data Centre: Cambridge, U.K.
(50) Frisch, M. J.; Trucks, G. W.; Schlegel, H. B.; Scuseria, G. E.; Robb, M. A.; Cheeseman, J. R.; Montgomery, J. A., Jr.; Vreven, T.; Kudin, K. N.; Burant, J. C.; Millam, J. M.; Iyengar, S. S.; Tomasi, J.; Barone, V.; Mennucci, B.; Cossi, M.; Scalmani, G.; Rega, N.; Petersson, G. A.; Nakatsuji, H.; Hada, M.; Ehara, M.; Toyota, K.; Fukuda, R.; Hasegawa, J.; Ishida, M.; Nakajima, T.; Honda, Y.; Kitao, O.; Nakai, H.; Klene, M.; Li, X.; Knox, J. E.; Hratchian, H. P.; Cross, J. B.; Bakken, V.; Adamo, C.; Jaramillo, J.; Gomperts, R.; Stratmann, R. E.; Yazyev, O.; Austin, A. J.; Cammi, R.; Pomelli, C.; Ochterski, J. W.; Ayala, P. Y.; Morokuma, K.; Voth, G. A.; Salvador, P.; Dannenberg, J. J.; Zakrzewski, V. G.; Dapprich, S.; Daniels, A. D.; Strain, M. C.; Farkas, O.; Malick, D. K.; Rabuck, A. D.; Raghavachari, K.; Foresman, J. B.; Ortiz, J. V.; Cui, Q.; Baboul, A. G.; Clifford, S.; Cioslowski, J.; Stefanov, B. B.; Liu, G.; Liashenko, A.; Piskorz, P.; Komaromi, I.; Martin, R. L.; Fox, D. J.; Keith, T.; Al-Laham, M. A.; Peng, C. Y.; Nanayakkara, A.; Challacombe, M.; Gill, P. M. W; Johnson, B.; Chen, W.; Wong, M. W.; Gonzalez, C.; Pople, J. A. *Gaussian 03*; Gaussian, Inc.: Wallingford, CT, 2004.